A Climatology of Easterly Wind Lake-Effect and Lake-Enhanced Precipitation Events over the Western Lake Superior Region Joshua D. Sandstrom<sup>1</sup>, Jason M. Cordeira<sup>2</sup>, Eric G. Hoffman<sup>2</sup>, and Nicholas D. Metz<sup>3</sup> 1: National Weather Service, Duluth, MN 2: Meteorology Program, Plymouth State University, Plymouth, NH 3: Dept. of Geoscience, Hobart and William Smith Colleges, Geneva, NY Submitted for consideration as an Article in the Journal of Applied Meteorology and Climatology Submitted: May 2022 Revisions Submitted: November 2022 and January 2023 Corresponding author address: Nicholas D. Metz Hobart and William Smith Colleges 300 Pulteney St. Geneva, NY 14456 Email: nmetz@hws.edu

### **Abstract**

Lake-effect precipitation is convective precipitation produced by relatively cold air passing over large and relatively warm bodies of water. This phenomenon most often occurs in North America over the southern and eastern shores of the Great Lakes, where high annual snowfalls and high-impact snowstorms frequently occur under prevailing west and northwest flow. Locally higher snow or rainfall amounts also occur due to lake-enhanced synoptic precipitation when conditionally unstable or neutrally stratified air is present in the lower troposphere. While likely less common, lake-effect and lake-enhanced precipitation can also occur with easterly winds, impacting the western shores of the Great Lakes. This study describes a 15-year climatology of easterly lake-effect (ELEfP) and lake-enhanced (ELEnP) precipitation (conjointly Easterly Lake Collective Precipitation: ELCP) events that developed in east-to-east-northeasterly flow over western Lake Superior from 2003 to 2018. ELCP occurs infrequently but often enough to have a notable climatological impact over western Lake Superior with an average of 14.6 events per year. The morphology favors both single shore-parallel ELEfP bands due to the convex western shoreline of Lake Superior and mixed-type banding due to ELEnP events occurring in association with "overrunning" synoptic-scale precipitation. ELEfP often occurs in association with a surface anticyclone to the north of Lake Superior. ELEnP typically features a similar northerly-displaced anticyclone and a surface cyclone located over the U.S. Upper Midwest that favor easterly boundary-layer winds over western Lake Superior.

#### 1. Introduction

Lake-effect (LEfP) and lake-enhanced (LEnP) precipitation (conjointly Lake Collective Precipitation: LCP) are known to cause significant sensible weather impacts across the Great Lakes Region, especially when it falls as snow. The cold-season climatology of synoptic-scale flow promotes "snowbelt" regions generally within 100 km of the southern and eastern shorelines of the Great Lakes that feature annual snowfall totals that are double the totals at nearby inland locations (e.g., Eichenlaub 1970). During anomalous flow patterns, the northern and western shores of the Great Lakes may also experience LCP events; however, their climatology is sparsely documented compared to those events occurring within the more typical "snowbelt" regions (e.g., Sanders 2017). The objectives of this study are to (1) document a climatology of LEfP and LEnP events that form in association with easterly winds (hereafter ELEfP and ELEnP; conjointly ELCP) over Lake Superior that may impact the "Twin Ports" region of Duluth, MN, and Superior, WI, and to (2) summarize the associated environmental characteristics favorable for ELCP.

LEfP is a type of mesoscale convective precipitation that forms when cold air flows over a relatively warmer body of water, such as the Great Lakes (AMS Glossary; Niziol et al. 1995; Laird et al. 2017). This precipitation often occurs in a post-cold frontal cold air advection regime with a westerly wind component, typically within 1–2 days after the passage of a cold front (Liu and Moore 2004). The cold air moving over the relatively warmer body of water causes the cold air to warm and moisten as sensible and latent heat is transferred into the air from the lake, which leads to static instability and may trigger convection. This convection may then form clouds and precipitation, which can take the form of shore-parallel bands (e.g., Laird et al. 2003; Steiger et al. 2013) or wind-parallel bands comprised of horizontal convective rolls (e.g., Kristovich 1993; Laird et al. 2003). LEfP can produce extreme snowfall totals in excess of 150 cm from a single lake-effect snow (LES) storm (Niziol et al. 1995) or produce persistent light precipitation with durations ranging from a few hours to several days. Extreme LES events are known to cause road and air traffic disruptions, property damage (including but not limited to roof collapses, structural failures, and tree damage), power outages, food and gas shortages, injuries, and death due to physical over-exertion and accidents (Kunkel et al 2002; NWS 2015). Flash flooding has also been documented from lake-effect rainbands (Nicosia et al. 1999). Locations within the LES snowbelt are often well-equipped to deal with heavy snow and its associated impacts (Schmidlin

1993). Alternatively, locations outside of the typical snowbelts, such as the western shores of the Great Lakes, may not be as well-equipped and might experience comparatively higher impacts.

The morphology of different types of LES bands is often the result of the direction of the prevailing lower-tropospheric winds relative to the orientation of the lake axes and the in-situ environmental characteristics. The different types of LES bands may be described as follows:

- Type I bands are single snow bands that develop parallel to the long axis of a lake, such as a west-to-east band extending across Lake Ontario (i.e., shore parallel bands; Niziol et al. 1995). These are typically the most intense snow bands, responsible for many of the extreme LES totals in the Great Lakes. These snow bands can produce snowfall rates as high as 30.5 cm (3 h)<sup>-1</sup> over the Tug Hill area east of Lake Ontario in association with bands driven by low-level convergence and ascent focused along the long-lake axis (Campbell and Steenburgh 2017).
- Type II bands are multiple parallel snow bands that form with winds flowing across the short axis of a lake. These cloud streets are typically weaker than Type I bands, but cover a greater area (i.e., wind-parallel bands).
- Type III bands form owing to the interaction of multiple lakes, such as a band initially forming over Lake Huron that extends across Lake Ontario (e.g., Lang et al. 2018).
- Type IV bands are shore-parallel bands that form in a cold environment with weak synoptic winds, usually due to land breeze convergence (e.g., Woolley et al. 1992).
- Type V bands are mesoscale vortices, which form in a similar environment as Type IV bands, but take the form of a mesoscale low-pressure system rather than a single band (e.g., Forbes and Merritt 1984; Grim et al. 2004).

The concave western lakeshore geometry of Lake Superior mirrors the eastern lakeshore geometries of Lakes Erie and Ontario, which favor Type I single banded precipitation under westerly winds. Of the five types of LES bands, it is hypothesized that Type I shore-parallel bands are likely to also develop in east-to-northeasterly flow over western Lake Superior that may subsequently produce LES in the Twin Ports region.

LEnP forms when low-pressure systems pass through the Great Lakes during cold air outbreaks and can contribute to enhanced snowfall concurrently with synoptically-forced precipitation (e.g., Brusky and Helman 1991; Lackmann et al. 2001; Owens et al. 2017). In many cases, LEnP may occur through the seeder-feeder mechanism. The seeder-feeder mechanism

135 involves precipitation falling from an upper-level cloud into a lower-level precipitating cloud 136 (AMS 2018). Although the seeder-feeder mechanism is commonly associated with synoptic-137 scale precipitation overlying orographic precipitation (e.g., Carruthers and Choularton 1983; 138 Purdy et al. 2005), it may also occur with synoptic-scale precipitation overlying non-orographic 139 precipitation forced by other mesoscale processes such as ocean-effect snowfall (e.g., 140 Waldstreicher 2002). In some cases, the presence of a seeder-feeder mechanism may also 141 influence precipitation type, increase precipitation efficiency and intensity, and result in 142 concomitant forecast errors (e.g., Schneider and Moneypenny 2002). It is hypothesized that 143 many ELEnP events may not occur without the presence of synoptic-scale precipitation (i.e., 144 lake-enhanced) or, if already developed, may occur in conjunction with heavier-than-expected 145 lake-effect precipitation or greater storm (both ELEnP and synoptic scale) total precipitation. An 146 example of the latter occurred in association with ~17 cm of ocean-effect snowfall and ~64 cm 147 of synoptic-scale snowfall in Portland, Maine, prior to and during a cyclone over the U.S. 148 Northeast in early February 2013 (M. Clair 2019, personal communication). The combined 149 snowfall totals resulted in a record storm-total snowfall that would not have occurred in the 150 absence of the ocean-effect snowfall. Additionally, ELEnP events that have produced high-151 impact snowfall accumulations have been observed along the western shores of Lake Michigan 152 (e.g., Brusky and Helman 1991; Owens et al. 2017), and similar setups likely occur along the 153 western shores of Lake Superior. 154 The frequencies, seasonality, and environmental conditions that support LEfP events 155 across the Great Lakes snowbelts are well known; however, the frequency, seasonality, and the 156 environmental conditions associated with ELEfP events are less understood. Currently, there is a 157 dearth of research on ELEfP events aside from a single case study of ocean-effect snow over 158 eastern Massachusetts by Waldstreicher (2002) and a preliminary five-year study of ELCP over 159 Lakes Ontario and Erie by Sanders (2017). Both pieces of research highlight the influence of 160 easterly flow ahead of an advancing region of low pressure and the presence of the seeder-feeder 161 precipitation-enhancement mechanism (e.g., Schneider and Moneypenny 2002) in the case of 162 ELEnP. While there are several case studies of ELEnP episodes (e.g., Brusky and Helman 1991; 163 Owens et al. 2017), climatological studies are sparse. This relative lack of previous studies

provide a unique opportunity to further study ELCP events by focusing over western Lake

Superior. The remainder of this paper is organized as follows. Section 2 details the data and

164

methods used in this study, while section 3 documents the frequency and seasonality of ELCP. Section 4 illustrates the primary synoptic and mesoscale atmospheric conditions for which ELCP occurs, and section 5 highlights two case studies. Finally, section 6 presents a summary of ELCP events off of Lake Superior and the ingredients pertinent to forecasting them.

### 2. Data and Methodology

Several methods and datasets were utilized to identify ELCP events for 15 cool seasons (September–May) spanning 2003–2004 through 2017–2018. First, a lower tropospheric wind climatology was created in order to identify easterly wind episodes over the western Lake Superior region. This wind climatology was generated by extracting 925-hPa wind data for a grid point located at 47°N, 91°W (Fig. 1) from the National Oceanic and Atmospheric Administration (NOAA) National Centers for Environmental Prediction (NCEP)-Climate Forecast System (CFS). The CFS is available as a reanalysis dataset spanning the period from 1 January 1979 to 31 March 2011 (Saha et al. 2006) and as an operational analysis dataset from 1 April 2011 to the present day (Saha et al. 2014) with 6-hourly temporal resolution. This grid point location was chosen because it is in close proximity to the Twin Ports and is the nearest over-water point in the 0.5-degree CFS dataset that could represent easterly flow over the lake with minimal impacts from local features such as land breezes and other coastal mesoscale circulations. Easterly wind episodes were identified for wind directions between 40 and 120 degrees (Fig. 1). This range was chosen to include all possible occurrences of easterly to east-northeasterly winds while allowing for slight variation in order to provide the greatest fetch for possible ELCP along the western shoreline of Lake Superior (i.e., directions outside of this range could potentially produce more overland wind trajectories; see Fig. 1). A total of 893 cool-season easterly wind episodes were identified using these criteria for any period of successive six-hour winds from the CFS data within the chosen directional range.

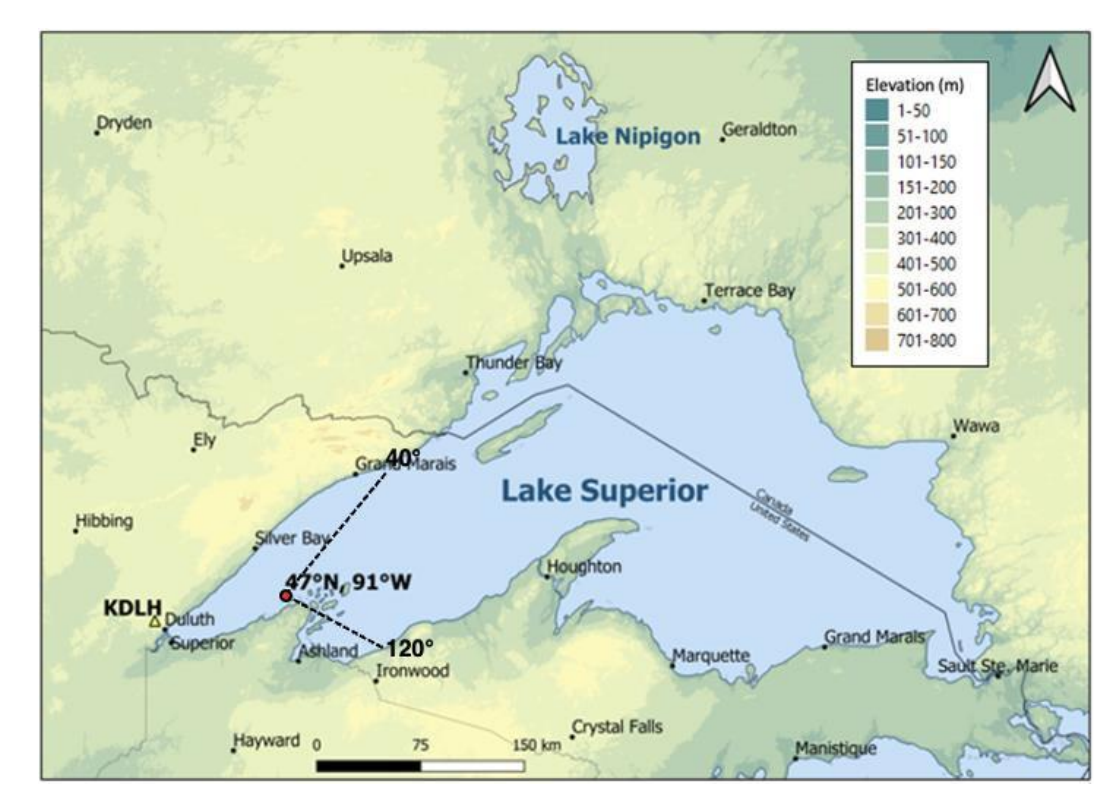


Figure 1. Topographic map of Lake Superior and surrounding areas. The locations of the KDLH radar site (yellow triangle) and the grid point location of 47°N, 91°W (red circle) are indicated on the map with the sector from 40° to 120° defined by dashed black lines. Background image source is from University of California Berkley Library. https://geodata.lib.berkeley.edu/catalog/stanford-zz225qj2166.

ELCP events were first visually identified via KDLH (Fig. 1) WSR-88D 0.5° base reflectivity imagery during easterly wind episodes. Radar data were analyzed using both the University Corporation for Atmospheric Research online imagery and Level-II radar data from the National Centers for Environmental Information using the NOAA Weather and Climate Toolkit to identify the presence of precipitation that resembled ELCP. The visual identification of presumptive ELCP events used specific criteria following the methodology of Laird et al. (2009):

- Precipitation appeared to move from Lake Superior towards the western shoreline of Lake Superior or remain nearly stationary over the lake.
- Precipitation was easily distinguishable from any synoptic precipitation in the area.
  Some synoptic precipitation events were classified as ELCP if they appeared to be lake-enhanced. Lake-enhanced precipitation is defined as synoptic precipitation that has some

enhancement along the periphery of the western shorelines of Lake Superior, coincident with an easterly wind episode.

 Any precipitation that resembled ELCP and had similar radar echoes nearby that did not originate over Lake Superior were either ignored or classified as "unknown"

A quality control process was also performed in order to positively identify the presumptive ELCP events. The first step of quality control evaluated the  $\Delta T$  between the lake water temperature and the 850-hPa air temperature at 47°N, 91°W using water temperatures from the Great Lakes Observing System Point Query Tool for the Great Lakes Coastal Forecasting System (GLCFS) and 850-hPa air temperatures from the CFS. These  $\Delta T$  values were calculated at 6-hr intervals for the period of GLCFS availability from 1 August 2008 through 31 May 2018. A presumptive ELCP event was positively identified if the ΔT value exceeded 13°C at some point during its duration, corresponding to a proxy for lake-effect convection and absolutely unstable static stability (e.g., Holroyd 1971). Presumptive ELCP events that failed the above mentioned test or occurred between 2003 and 2007 (prior to CLCFS availability) were compared against NWS Duluth Area Forecast Discussions. If "lake-effect" or "lake-enhanced precipitation" were mentioned prior to the presumptive ELCP event, the event was positively identified as ELCP. Seven presumptive ELCP events classified as "unknown" were removed after further investigation of nearby atmospheric soundings, surface observations, and dualpolarization radar revealed these events to be bright banding, land breeze convergence, nonmeteorological echoes, or orographic/synoptic in origin. In total there were 219 ELCP events.

ELCP events were further classified by their band types (i.e., morphology) and association with synoptic precipitation (i.e., ELEfP and ELEnP). Band type classification followed the methodology of Niziol (1995) with minor modifications. For example, mesoscale vortices and shore-parallel band (lake-breeze) classifications were omitted because very few events (n=3; ~1.4%) fit those criteria. Further, a cellular convection category was added along with a classification for mixed-band type in order to account for ELCP events that transitioned between band types. The resulting band types in this study include: SB – single band; MB – multiple bands; WNB – widespread/non-banded; CC – cellular convection; and MiB – mixed-band (Table 1). ELCP is further classified as Type A if it occurred independent of synoptic precipitation (i.e., ELEfP) and Type B if it occurred in association with synoptic precipitation or lake-enhanced precipitation (i.e., ELEnP; Table 1). ELEnP events that began independent of, but

ended with synoptic precipitation were classified as Type A-to-B and oppositely Type B-to-A. The former is referred to as a predecessor ELEnP event and the latter is referred to as a successor ELEnP event. Events that had multiple synoptic interactions (e.g., Type A-to-B-to-A) were classified separately as mixed-synoptic interaction.

Table 1: Summary of ELCP band type classification, synoptic-associated precipitation classification, frequency of occurrence, and percentage of total events

Band Type Classific	Frequency (Percentage)			
SB:	Single Band	60 (27.4%)		
MB:	Multiple Bands	7 (3.2%)		
WNB:	Widespread, Non-banded	49 (22.4%)		
CC:	Cellular Convection	6 (2.7%)		
MiB:	Mixed-band	97 (44.3%)		
Precipitation Classi	fication			
Type A:	Independent of synoptic-scale precipitation	57 (26.0%)		
Type B:	Associated with synoptic-scale precipitation	66 (31.1%)		
Type A-to-B:	Began without, ended with synoptic-scale precipitation	27 (12.3%)		
Type B-to-A:	Began with, ended without synoptic-scale precipitation	39 (17.8%)		

Finally, ELCP events were classified by their association with warm and cold air advection, as it is hypothesized that many ELEnP events may occur with warm air advection and ELEfP events are likely associated with cold air advection. Upper air temperature and wind maps at the 925-hPa, 850-hPa, and 700-hPa levels were visually analyzed for warm, cold, or neutral temperature advection for each ELCP event (Table 2). A single time was chosen for analysis closest to the midpoint of each ELCP event, and for instances where two times were equitemporal from the midpoint, one was decided such that 925-hPa winds were closest to onshore (e.g., east-northeasterly).

Table 2: Summary of a) ELCP and b) ELEfP events associated with cold air advection, warm air advection, and neutral temperature advection at 925 hPa, 850 hPa, and 700 hPa pressure levels. Data was derived from Plymouth State weather archive.

a. ELCP Events	925 hPa Frequency	850 hPa Frequency	700 hPa Frequency		
	(Percentage)	(Percentage)	(Percentage)		
Cold Air Advection	127 (58.0%)	107 (48.9%)	94 (42.9%)		
Warm Air Advection	50 (22.8%)	65 (29.7%)	62 (28.3%)		
Neutral Advection	42 (19.2%)	47 (21.4%)	63 (28.8%)		

b. ELEfP Events	925 hPa Frequency	850 hPa Frequency	700 hPa Frequency		
	(Percentage)	(Percentage)	(Percentage)		
Cold Air Advection	41 (72.0%)	35 (61.4%)	32 (56.1%)		
Warm Air Advection	8 (14.0%)	10 (17.5%)	6 (10.6%)		
Neutral Advection	8 (14.0%)	12 (21.1%)	19 (33.3%)		

306

307

308

309

310

311

312

313

314

315

316

317

318

319

320

321

322

323

324

325

326

327

328

329

## 3. Results: ELCP climatology

The wind climatology yielded 893 cool-season easterly wind episodes over western Lake Superior that produced 219 total ELCP events. Thus, ELCP was present ~24.5% of the time during the cool season when an easterly wind episode was noted. The annual average frequency is 14.6 ELCP events per year, with a range of seven ELCP events during the cool season of 2011–2012 to 23 ELCP events during the cool season of 2010–2011 (Fig. 2a). Of the 219 ELCP events, there were 57 ELEfP events. ELEfP was present ~6.4% of the time during the cool season with an easterly wind. The annual average frequency is 3.8 ELEfP events per year, with a range of 1 ELEfP event during the cool seasons of 2011-2012 and 2016-2017 to seven ELEfP events during the cool season of 2004-2005 (Fig. 2a). The monthly frequency maximum in easterly wind episodes occurs during March through May, whereas the monthly frequency maximum in ELCP and ELEfP spans December through February (Fig. 2b). The monthly frequency maximum in easterly wind episodes during the spring months could be caused by lake breezes, and is generally not associated with ELCP due the statically stable environment produced by warmer air temperatures overlying colder lake water temperatures. The monthly frequency of easterly wind episodes is smallest during winter months when the monthly frequency of ELCP events is largest. ELCP/ELEfP events occur ~58% and ~13% of the time, respectively, that there is an easterly wind episode during this period (Fig. 2b). This result suggests that easterly wind episodes are relatively rare during the middle of the cool season, but their occurrence often leads to ELCP events. The mean duration of ELCP events is ~21 hours with a distribution that varies considerably with the shortest event duration of approximately one hour and the longest event duration of 122 hours (Fig. 2c). The mean duration of ELEfP events is ~18 hours with a distribution of durations that vary from approximately 2 hours to 39 hours. A majority of ELCP and ELEfP events lasted 10 to 20 hours with longer duration events skewing the mean toward longer durations.

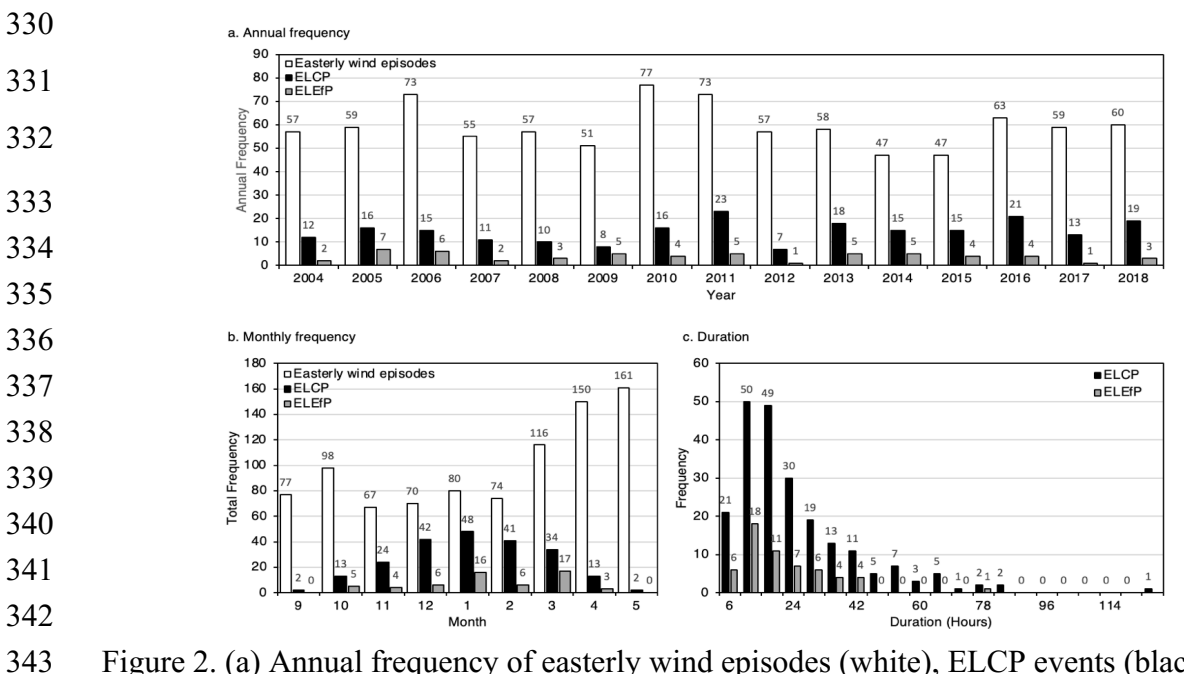


Figure 2. (a) Annual frequency of easterly wind episodes (white), ELCP events (black), and ELEfP events (grey) (b) monthly total frequency easterly wind episodes (white), ELCP events (black), and ELEfP events (grey), and (c) histogram of duration of ELCP events (black) and ELEfP events (grey) over western Lake Superior.

A large majority of ELCP events over western Lake Superior occur during the winter months of December through February (Fig. 2b) when the average difference ( $\Delta T$ ) between the lake water temperature and 850-hPa air temperature is between 10.0°C and 14.2°C (i.e., conditionally or absolutely unstable; Fig. 3). The  $\Delta T$  is >13°C for more than half of the events in December from 2008-2018. A weakly unstable lower atmosphere (i.e., Lake-to 850  $\Delta T$  between 4°C and 10°C) that may be marginally favorable for ELEnP or light ELEfP (particularly with a boundary layer shallower than 850 hPa) was present for all but one of the remainder of ELCP events. ELCP events become less frequent into April, despite an increase in easterly wind episodes, as increasing air temperatures and persistent cold water temperatures means that lake-effect precipitation is less likely to occur. Ice cover over western Lake Superior is also climatologically highest during February and March (Wang et al. 2017), and this may lessen the frequency of ELCP (e.g., Cordeira and Laird 2008).

	s	SSW	SW	wsw	W	WNW	NW	NNW	N	NNE	NE	ENE	Е	ESE	SE	SSE
Jul	-0.2	0.2	0.2	0.7	2.5	2.8	2.7	4.0	3.8	4.7	3.7	4.0	2.3	2.6	2.2	1.7
Aug	3.1	1.8	1.6	1.4	4.4	5.1	5.9	6.1	6.0	5.6	5.4	5.0	4.6	3.3	3.6	2.1
Sep	2.5	1.1	1.9	2.5	5.4	6.1	7.9	9.0	9.2	6.1	5.0	5.6	3.4	3.2	2.9	2.3
Oct	2.4	1.8	3.0	4.1	8.2	9.1	9.6	10.1	9.9	8.0	8.3	6.4	5.5	5.5	5.2	2.8
Nov	3.9	6.2	4.9	7.1	10.0	11.4	14.8	15.0	14.4	11.6	10.4	10.1	10.0	7.9	6.7	4.8
Dec	9.8	10.5	10.6	10.4	16.4	19.3	17.9	17.9	15.6	15.0	14.5	14.2	13.6	12.9	10.8	12.7
Jan	10.2	10.9	10.2	9.4	13.8	17.3	19.0	18.0	18.3	17.4	16.9	13.9	11.6	9.3	6.8	9.0
Feb	7.2	7.7	8.0	9.7	12.2	14.0	16.3	16.8	14.6	14.4	12.4	11.5	11.0	10.5	6.6	8.2
Mar	0.9	1.3	3.5	4.6	4.9	9.6	12.2	11.3	10.5	8.1	10.7	8.7	5.2	3.2	4.1	3.7
Apr	0.6	-1.1	-0.2	0.7	3.2	4.8	7.2	7.4	6.4	6.5	5.0	4.6	3.0	1.5	1.1	0.9
May	-4.4	-4.5	-2.9	-2.1	0.7	1.2	3.1	3.1	3.5	3.2	2.6	0.6	-2.0	-2.0	-1.6	-3.4
Jun	-2.8	-3.9	-1.7	-1.7	-0.8	0.7	1.3	1.7	3.1	0.7	3.0	0.8	-1.0	-1.3	-1.0	-2.4

Figure 3. Monthly average difference ( $\Delta T$ ) between Lake Superior water temperatures and 850-hPa temperature by month and wind direction for August 2008 – May 2018 at 47°N, 91°W. Lake water temperatures were obtained from the GLCFS and 850-hPa temperatures were obtained from the CFSR and GFSR datasets. Orange-shaded cells indicate  $\Delta T \ge 13$ °C (absolutely unstable; favorable for ELEfP), yellow-shaded cells indicate a  $\Delta T$  that is  $\ge 10$ °C and < 13°C (conditionally unstable; favorable for ELCP and marginally favorable for ELEfP), non-shaded cells indicate a  $\Delta T$  that is  $\ge 4$ °C and < 10°C (stable or weakly unstable; marginal for ELCP), and blue-shaded cells indicate  $\Delta T < 4$ °C (stable; not favorable for ELCP).

Approximately half (n=111; ~50%) of ELCP events occurred in association with KDLH METAR reports of light snow (Table 3). Of all ELEfP events when precipitation was observed at KDLH, 29 events (~93.5%) were light snow. There were fewer ELCP events that occurred in association with moderate snow (n=19), heavy snow (n=9), rain/drizzle (n=11), or mixed precipitation (e.g., precipitation types not already mentioned or transitions between precipitation types, including rain, freezing rain, drizzle, freezing drizzle, ice pellets, snow, or unknown precipitation; n=25). The greatest intensity of precipitation observed in an event's duration determined its intensity classification. A large number of ELCP events (n=44) also occurred in association with no reported precipitation at KDLH. These latter non-precipitating events indicate that the area of precipitation associated with the ELCP either never made landfall or made landfall at a location away from the KDLH site. There were some ELCP events in which the region of ELCP did not affect KDLH directly, but synoptic precipitation was still recorded. Thus, there are some instances for which precipitation intensity is not necessarily representative of the region of ELCP. The precipitation type still provides useful guidance as to what type of precipitation occurred during the ELCP event. For example, the dominant precipitation type associated with ELCP events during autumn is either rain or a rain and snow mix (Table 3). Further, the majority of ELCP events in November and December occurred in association with snow and was almost exclusively snow for ELCP events in January through March.

Table 3. Frequency of precipitation types and intensities by month recorded in KDLH METAR reports during each ELCP/ELEfP event.

Precipitation	Sep	Oct	Nov	Dec	Jan	Feb	Mar	Apr	May	Total
Type/Intensity										
Light Snow	0/0	0/0	13/2	17/4	31/9	27/4	20/10	3/0	0/0	111/29
Moderate Snow	0/0	0/0	2/0	2/0	3/0	3/0	5/0	3/0	1/0	19/0
Heavy Snow	0/0	0/0	0/0	3/0	1/0	3/0	1/0	1/0	0/0	9/0
Mixed	0/0	0/0	0/0	9/0	2/0	4/0	0/0	1/0	0/0	16/0
Precipitation										
Rain and Snow	0/0	2/1	1/0	3/0	0/0	0/0	0/0	2/0	1/0	9/1
Rain or Drizzle	1/0	5/0	4/1	1/0	0/0	0/0	0/0	0/0	0/0	11/1
Any Type (Sum)	1/0	7/1	20/3	35/4	37/9	37/4	26/10	10/0	2/0	175/31
No Precipitation	1/0	6/4	4/1	7/2	11/7	4/2	8/7	3/3	0/0	44/26

Most (~58%) ELCP events were associated with cold air advection at 925 hPa, while the remainder were associated with neutral or warm air advection (Table 2a). There was comparatively higher cold air advection at 925 hPa versus aloft and comparatively higher warm air advection aloft (850 hPa and 700 hPa) versus at 925 hPa. This result may be representative of ELEnP events that often feature elevated warm air advection atop cold air advection (e.g., warm frontal synoptic precipitation). ELEfP events had a higher percentage of cold air advection at 925-hPa (72%), and comparatively less frequent warm air advection aloft (Table 2b). These data suggest that ELCP events frequently feature cold air advection, which is expected especially for ELEfP events, but also that warm air advection is frequently associated with ELEnP events.

### 4. Results: Band morphology and classification

a. ELCP morphology

Examples of the different band types observed during ELCP events over western Lake Superior are included in Figure 4. Distinguishing between band type morphology may provide useful information regarding the environmental characteristics that led to the formation of ELCP (Niziol 1987). For example, organized banded structures (e.g., SB or MB events in Figs. 4a,b) are more likely to occur in environments characterized by weak or no directional wind shear with height as opposed to disorganized or widespread precipitation (e.g., WNB events in Fig. 4c) that are more likely to occur in an environment characterized by stronger wind shear (Niziol 1987).

Similar to the convex eastern coastlines of Lake Erie and Lake Ontario with lake-effect that develops under westerly flow, the convex western coastline of Lake Superior (Fig. 1) also favors single bands (e.g., Fig. 4a) with 60 identified SB ELCP events. WNB ELCP events were also common (n=49) and appeared on radar as stratiform precipitation that contained convective elements (e.g., Fig. 4c). This type of precipitation is generally disorganized and likely occurred in association with substantial directional wind shear (e.g., >30 degrees) in the convective layer (e.g., Niziol 1987). There were far fewer MB events (n=7; e.g., Fig. 4b) and CC (n=6; Fig. 4d) events. There were 97 mixed-type bands that involved transitions between band types, primarily associated with a SB event transitioning to or from another type. Most of these mixed-type events exhibited only one transition during their lifecycle, but some transitioned three or four times before ending (e.g., Fig. 4e). Some bands transitioned from a SB event to a lake-enhanced precipitation event with no organized banded structure (e.g., Fig. 5c), or alternatively began as a widespread precipitation event with locally enhanced ELCP that transitioned to a SB event (e.g., Fig. 5d). In summary, two band types occurred most frequently (e.g., SB and WNB) and there are many events that involved transitions between different band types.

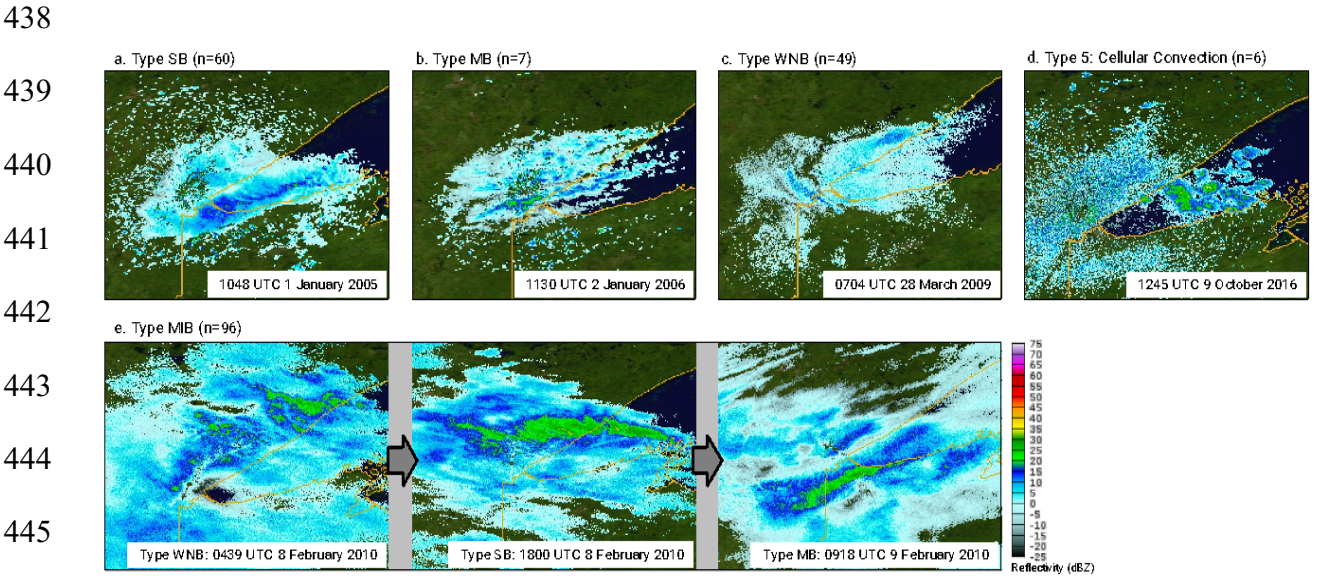


Figure 4. Duluth (KDLH), MN, WSR-88D 0.5-degree reflectivity of ELCP band morphology types and counts over western Lake Superior: (a) Type SB on 1 January 2005; (b) Type MB on 2 January 2006; (c) Type WNB on 28 March 2009; (d), Type CC on 9 October 2016; and (e) Type MiB, including Type WNB, Type SB, and Type MB on 8–9 February 2010. Analyses are adapted from imagery retrieved from the National Centers for Environmental Information online and visualized using the NOAA Weather and Climate Toolkit.

a. ELCP with and without synoptic-scale precipitation (i.e., ELEfP and ELEnP)

 This section illustrates composite analyses of ELCP events that occur without (Type A; Fig. 5a) or with (Type B; Fig. 5b) synoptic-scale precipitation. ELCP events may transition between Type A and Type B events, including both predecessor ELEnP events (Type A-to-B; Fig. 5c) and successor ELEnP events (Type B-to-A; Fig. 5d). The count and percentages of each type are as follows: Type A (n=57; 26.0%), Type B (n=66; 30.1%), Type A-to-B (n=27; 12.3%), and Type B-to-A (n=39; 16.9%). There were 30 ELCP events (13.7%) that could not be classified using the scheme above. These events occurred in association with multiple transitions involving synoptic-scale precipitation throughout the duration of an event and were deemed inappropriate for subsequent composite analysis.

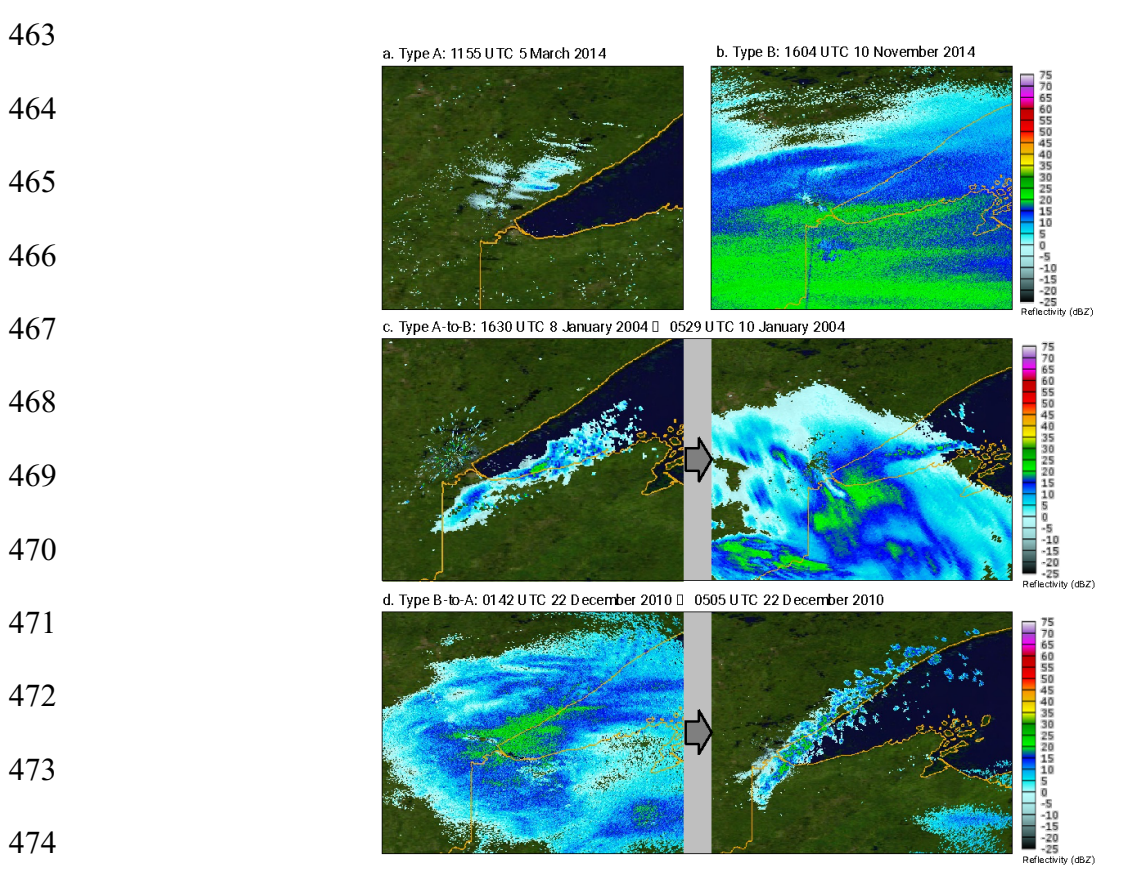


Figure 5. Duluth (KDLH), MN, WSR-88D 0.5-degree reflectivity examples of (a) Type A ELEfP on 5 March 2014, (b) Type B ELEnP on 10 November 2014, (c) Type A-to-B with a transition to synoptic-scale precipitation (i.e., predecessor ELEnP) on 8–10 January 2004, and (d) Type B-to-A with a transition to no synoptic-scale precipitation (i.e., successor ELEnP) on 22 December 2010. Analyses are adapted from imagery retrieved from the National Centers for Environmental Information online and visualized using the NOAA Weather and Climate Toolkit.

Composite analysis of the Type A ELEfP events illustrates that they occur in association with an anomalously strong anticyclone with positive SLP anomalies in excess of 7 hPa over southern Canada and over the U.S. Upper Midwest (Fig. 6a) situated between a broad 500-hPa ridge over western North America and trough over eastern North America (Fig. 6b). The placement of the surface anticyclone to the northwest of Lake Superior is consistent with the lower tropospheric east-to-northeasterly geostrophic flow that was used to identify easterly wind episodes and ELEfP events. Composite analysis of the Type B ELEnP events illustrates that the synoptic-scale precipitation events occur in association with an anomalously strong anticyclone with positive SLP anomalies greater than 5 hPa over southern Canada and an anomalously strong cyclone with negative SLP anomalies less than -5 hPa over the U.S. Central Plains (Fig. 6c). These surface features occur within quasi-zonal flow at 500-hPa across North America with a short-wave trough (e.g., Metz et al. 2019) over the U.S. Intermountain West and shortwave ridge over the Great Lakes Region (Fig. 6d). The placement of the cyclone and anticyclone straddling Lake Superior is also consistent with the lower tropospheric east-to-northeasterly geostrophic flow that was used to identify easterly wind episodes and ELEnP events. The composite synoptic-scale patterns suggest that Type B ELEnP events occur in the relatively cold easterly flow north of a surface warm front and potentially beneath "overrunning" synoptic-scale precipitation related to the development of a cyclone over the U.S. Central Plains downstream of a mid-tropospheric shortwave trough (Figs. 6c,d). In this case, it is hypothesized that synopticscale precipitation may be seeding the lower-tropospheric precipitation processes within the convective-layer ELEnP as shown in Waldstreicher (2000) and Figure 5b.

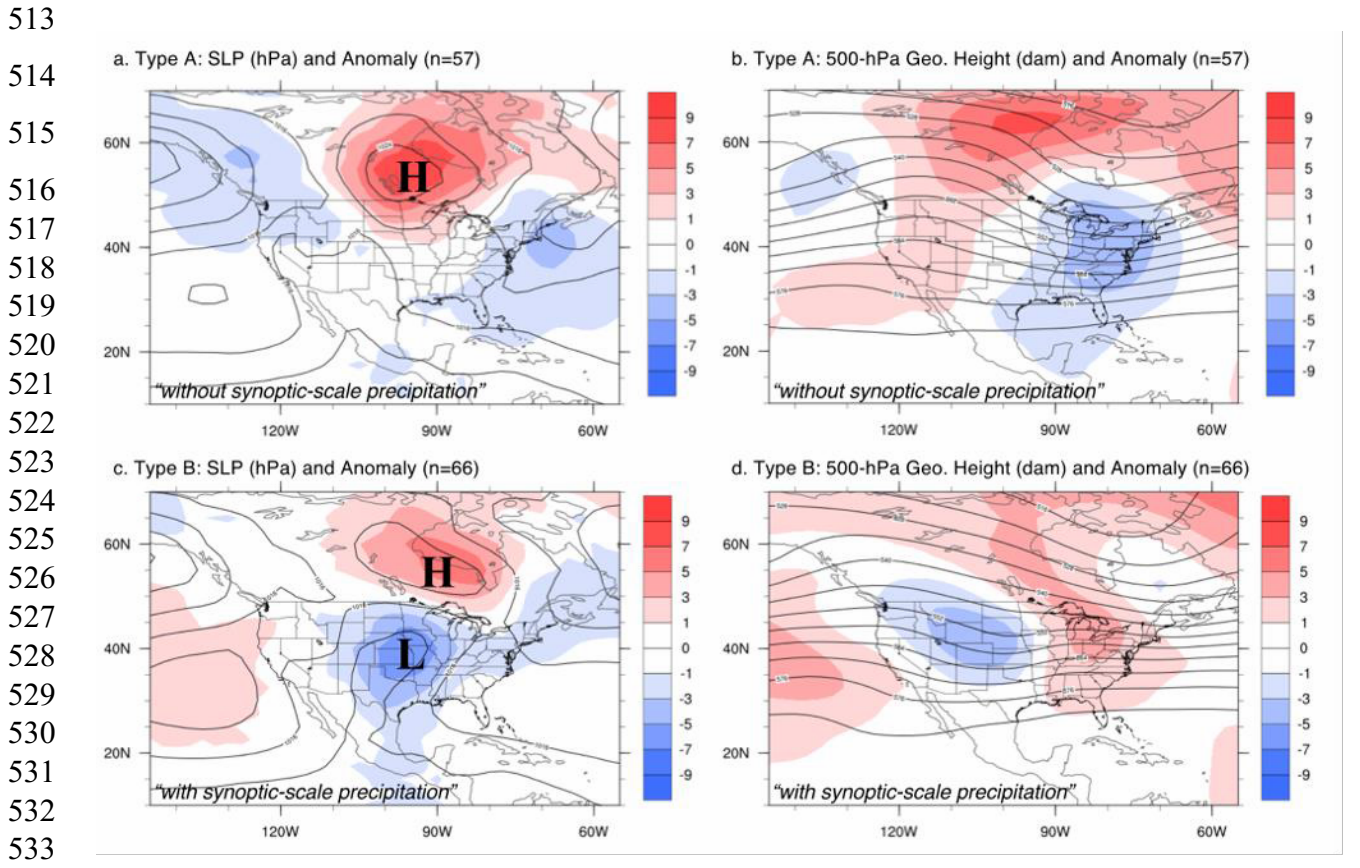


Figure 6. Composite analyses of (a, c) SLP (hPa; contours) and SLP anomaly (hPa; shaded according to scale) and (b, d) 500-hPa geopotential height (dam; contours) and geopotential height anomaly (dam; shaded according to scale) for ELCP events classified as (a,b) Type A without synoptic-scale precipitation (i.e., ELEfP) and (c,d) Type B with synoptic scale precipitation (i.e., ELEnP). Anomalies are calculated as departures from a 21-day climatology following the methodology of Hart and Grumm (2001) for a period of 1979 – 2008 using data from the NCEP – NCAR reanalysis.

Composite analysis of the Type A-to-B ELEnP events illustrates several synoptic-scale patterns that are similar to both Type A and Type B events with an anomalously strong surface anticyclone over southern Canada and an anomalously strong cyclone over the U.S. Central Plains (Fig. 7a). Given that these events transition to become more like Type B ELEnP events, it is likely that these events develop in association with static instability under geostrophic easterly flow associated with the surface anticyclone and later become collocated with overrunning synoptic-scale precipitation in conjunction with the northward propagation of the Central Plains cyclone. Alternatively, composite analysis of the 39 Type B-to-A ELEnP events illustrate a well-defined anticyclone with positive SLP anomalies over southern Canada and only weakly negative SLP anomalies over the U.S. Central Plains (Fig. 7c). These events occur with a highly

amplified mid-tropospheric flow pattern with a 500-hPa ridge over western North America and trough over eastern North America (Fig. 7d). Given that these events transition to become more like Type A events, it is likely that these events develop in association with easterly flow to the north of weak low pressure over the western Great Lakes region and are maintained as non-synoptic precipitation ELEfP as an anticyclone propagates eastward across southern Canada. In all four types, ELCP is influenced by the presence of an anomalously strong surface anticyclone over southern Canada that is likely responsible for either the formation or maintenance of ELCP in the presence of or lack of synoptic-scale precipitation related to a surface cyclone over the U.S. Central Plains.

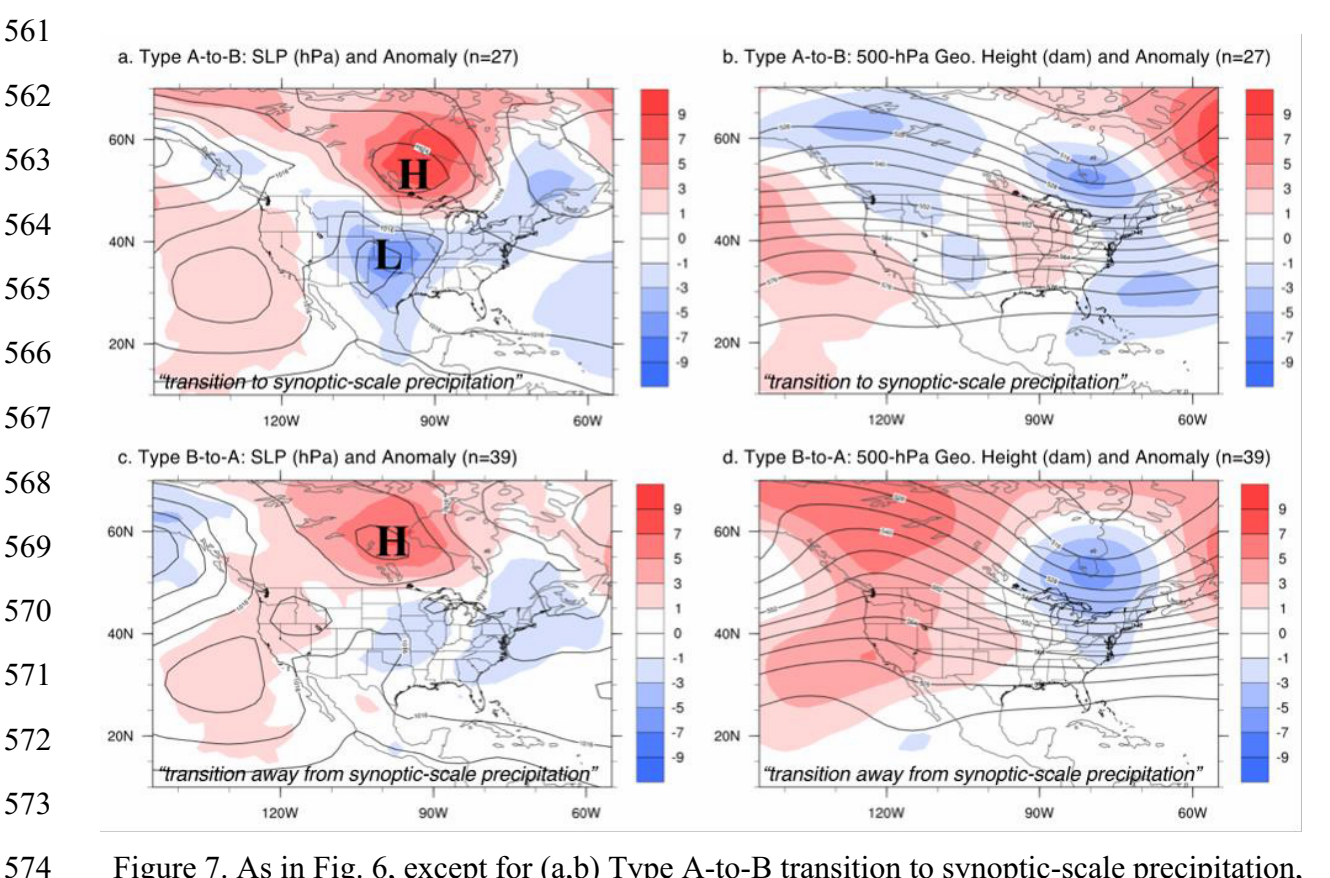


Figure 7. As in Fig. 6, except for (a,b) Type A-to-B transition to synoptic-scale precipitation, and (c,d) Type B-to-A transition to no synoptic-scale precipitation.

### 5. Results: Case Studies – 6 February 2008 and 4 December 2007

Two case studies are presented below. The first (6 February 2008) provides an example of a "typical" ELEfP event with limited impacts. The second (4 December 2007) provides an example of a high-impact ELEnP event. These case studies provide a small sample of the results

as described above (e.g., band type variation, synoptic versus no-synoptic precipitation interaction, band type transitions, and variation of synoptic features).

# a. 6 February 2008 – Low-impact light snow event

A SB ELEfP event occurred over western Lake Superior at 0200 UTC 6 February 2016 (Fig. 8a). The SB made landfall and was producing snow over the Twin Ports area as of 0505 UTC (Fig. 8b). Over the next several hours, the SB transitioned to a WNB type with more widespread and generally less intense radar echoes (Fig. 8c). The WNB ELEfP meandered about the western Lake Superior shoreline throughout the day, eventually weakening in intensity during the afternoon (Fig. 8d) and terminating during the early evening (not shown).

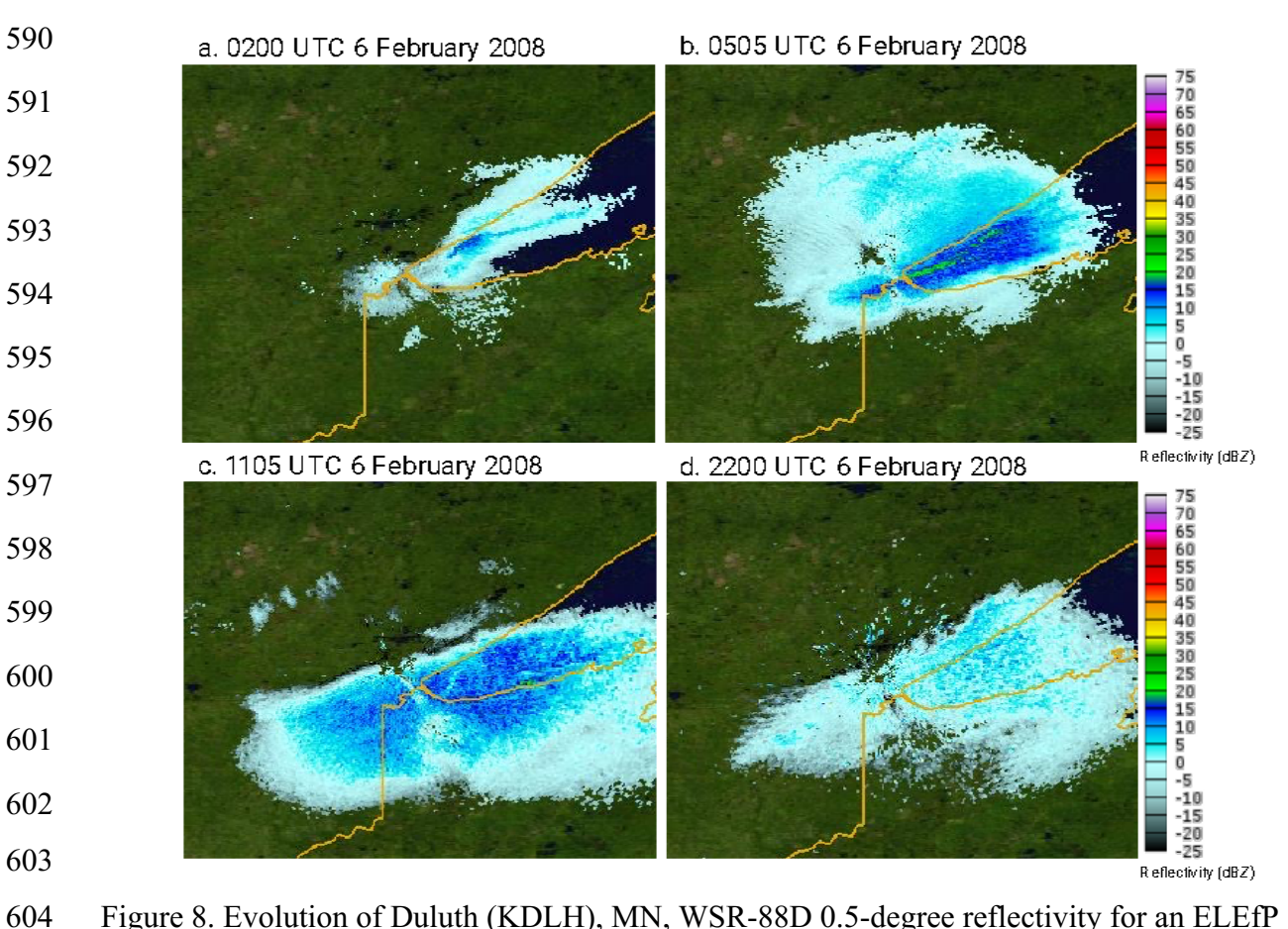


Figure 8. Evolution of Duluth (KDLH), MN, WSR-88D 0.5-degree reflectivity for an ELEfP event on 5-6 February 2008 at (a) 0200 UTC 6 February, (b) 0505 UTC 6 February, (c) 1105 UTC 6 February, and (d) 2200 UTC 6 February. Analyses are adapted from imagery retrieved from the National Centers for Environmental Information online and visualized using the NOAA Weather and Climate Toolkit.

This event developed in association with surface high pressure centered over northern

Ontario (not shown; NOAA 2022), which provided sufficient cold air for convective instability over western Lake Superior and northeasterly winds that brought light snow to the Twin Ports area. The event terminated as high pressure drifted east into Quebec and surface winds shifted to southerly (not shown; NOAA 2022). Snowfall remained light throughout the event, with observed snowfall amounts less than 5 cm (2 in; Iowa State University 2022). Several features may have limited the intensity of the ELEfP, including marginally favorable lake-to-850  $\Delta T$ , minimized dendrite growth, dry air intrusion towards the end of the event, and partial ice cover over western Lake Superior (Iowa State University 2022; GLERL 2022). Towards the end of the event, the lake-modified layer was shallow and topped at ~876 hPa (Fig. 9), favoring the light snow as observed.

611

612

613

614

615

616

617

618

619

620

621

623

624

627

628 629

630 631

632

633

634

635

636

637

638

639

640

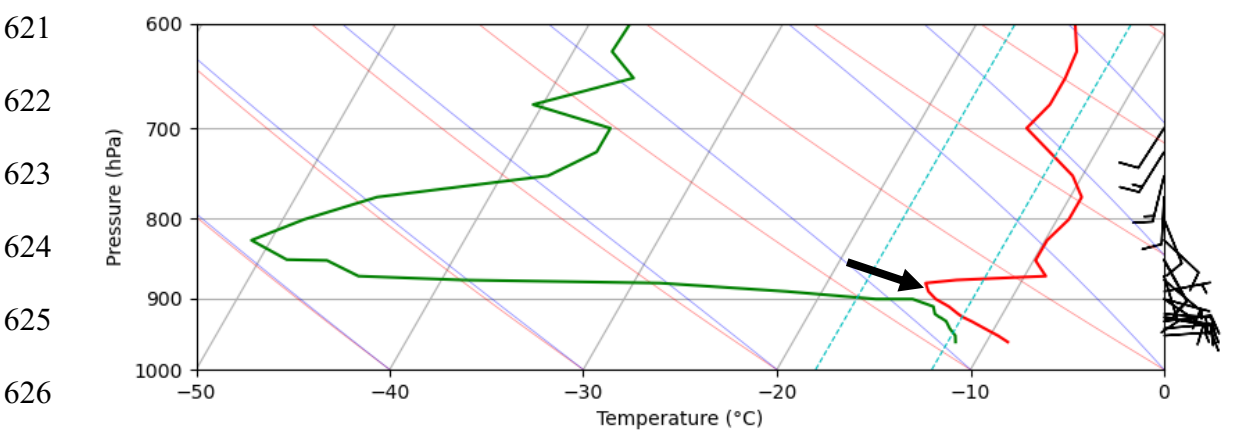


Figure 9. AMDAR aircraft-derived descent sounding at KDLH Airport at 2024 UTC 6 February 2008. The green line represents the dewpoint temperature and the red line represents the temperature. Blue dashed lines represent -12°C and -18°C isotherms indicative of the dendritic growth zone. The black arrow denotes a temperature inversion at ~876-hPa. Source: NOAA AMDAR page. Soundings were created using METPY (May et al. 2022).

This case study highlights a "typical" ELCP event that produced light snowfall amounts. Surface high pressure north of Lake Superior is consistent with the climatology for Type A ELEfP events (e.g., Fig. 6a). Dry air associated with high pressure was likely a factor in producing light snowfall (Iowa State University 2022), and is consistent with the predominantly light precipitation observed with ELEfP events (Table 3). A transition from SB to WNB band types in this case is also representative of the majority of ELCP events observed, and vertical wind shear in the surface-to-876 hPa lake-modified layer in the latter part of the event (Fig. 9) may have contributed to the transition to WNB (e.g., Fig. 4c). While light snowfall events such

as this are common in the western Lake Superior region (Table 3), including the Twin Ports, even light snow can create hazardous driving conditions, especially in snow squalls with localized white-out conditions (DeVoir 2004).

### b. 4 December 2007 – High-impact heavy snow event

This case study reviews a notable ELEnP event that occurred in association with Type A-to-B-to-A ELEnP event, involving a transition from a SB event to a synoptic-scale enhanced precipitation event (i.e., predecessor event) on 4–5 December 2007. The event terminated as a SB (i.e., successor event). The event produced up to 43 cm (17 in.) of snow over the Twin Ports region (Figs. 10a,b) and illustrates (1) the ELEnP SB band type, (2) ELCP snow band characteristics with and without synoptic-scale precipitation, (3) analyses representative of the aforementioned composite analyses, and (4) a high-impact snowfall event that resulted in traffic disruptions.

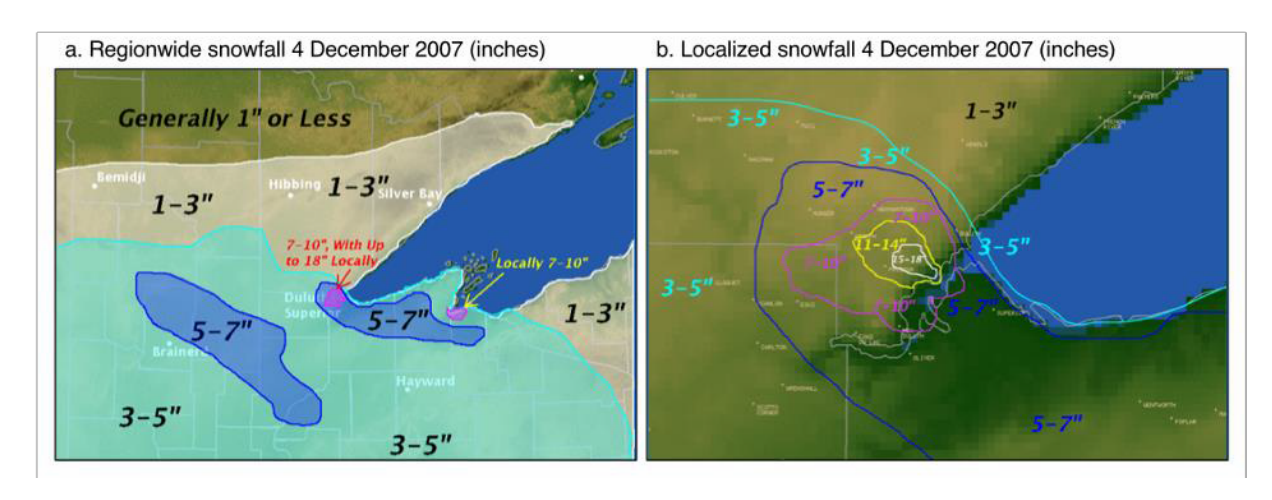


Figure 10. Snowfall analyses prepared by the Duluth, MN, National Weather Service Weather Forecast Office of (a) regional snowfall (inches) and (b) localized snowfall (inches) in the Twin Ports area for 4 December 2007.

A predecessor SB ELEfP event was located over western Lake Superior at 0556 UTC on 4 December 2007 (Fig. 11a) that slowly propagated westward overnight and moved inland, impacting the Twin Ports area by 0901 UTC (Fig. 11b). At this time, a broad area of synoptic snowfall also began to overspread central and northern Minnesota. The ELEnP band intensified during the morning and afternoon hours as synoptic-scale snowfall increased over Northeast Minnesota; Reflectivity in the ELEnP band increased to >20–30 dBZ between 1305 UTC and

1708 UTC with heavy snow reported at the Duluth International Airport (KDLH; Ogimet 2019) and snowfall rates >5 cm h<sup>-1</sup> (Iowa State University 2019; Figs. 11c,d). Throughout the afternoon, the ELEnP band maintained its SB characteristics as a narrow but intense area of heavy snow embedded within widespread synoptic-scale precipitation and persisted through 1904 UTC (Fig. 11e). The embedded snow band remained over the Twin Ports area until about 0227 UTC 5 December 2007 when it began to drift south along the south shore of Lake Superior (Fig. 11f). The snow band became isolated (i.e., ELEfP) and weakened at around 0622 UTC after synoptic precipitation ended later that evening (not shown).

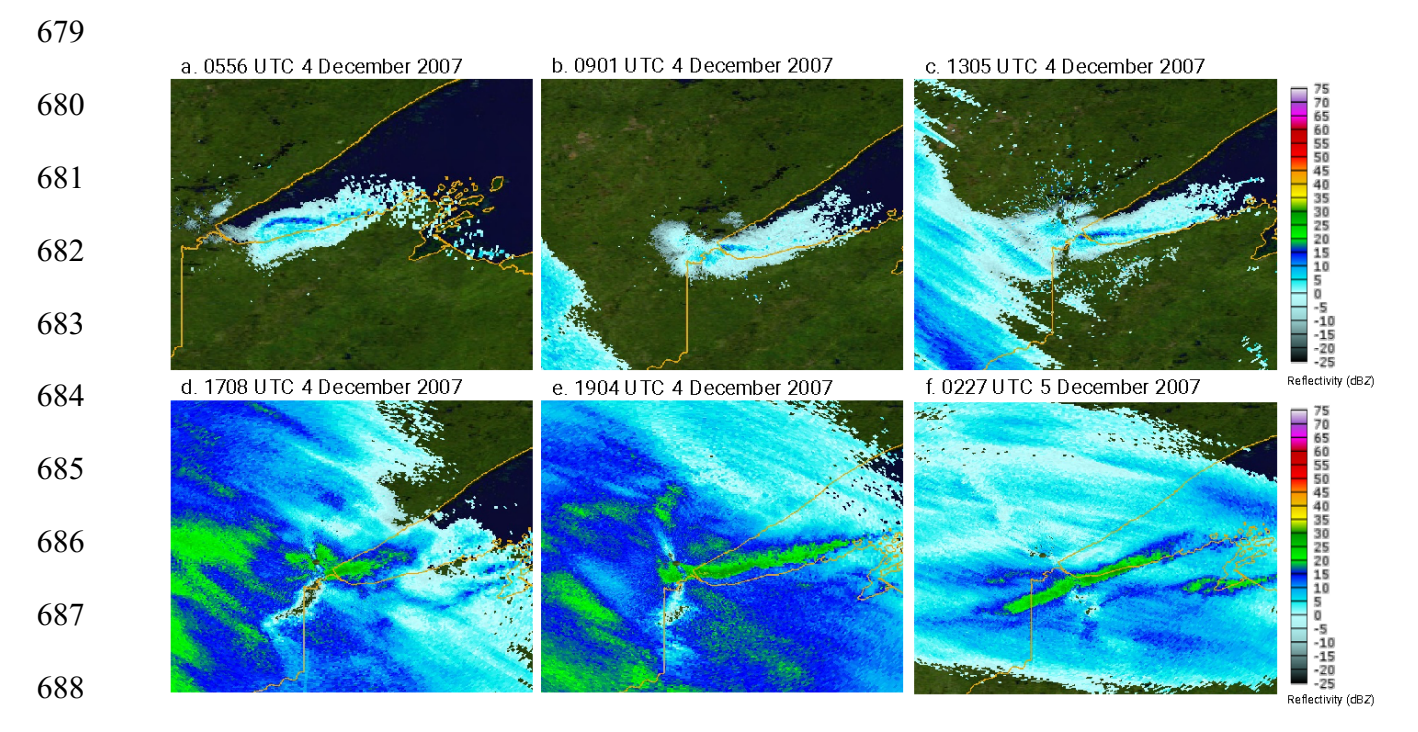


Figure 11. Evolution of Duluth (KDLH), MN, WSR-88D 0.5-degree reflectivity for an ELEnP event on 4–5 December 2007 at (a) 0556 UTC 4 December, (b) 0901 UTC 4 December, (c) 1305 UTC December, (d) 1708 UTC 4 December, (e) 1904 UTC 4 December and (f) 0227 UTC 5 December. Analyses are adapted from imagery retrieved from the National Centers for Environmental Information online and visualized using the NOAA Weather and Climate Toolkit

The ELEnP developed within a synoptic-scale environment characterized by a 70 m s<sup>-1</sup> upper-tropospheric jet streak at 250-hPa at 1800 UTC within broad northwesterly flow across the U.S. Central Plains (Figs. 12a,b). This northwesterly flow aloft paralleled a strong lower-tropospheric temperature gradient at 700 hPa and 850 hPa that bifurcated the Northern Plains (Figs. 12c,d). A 700-hPa trough and 850-hPa closed low with an attendant surface cyclone

located over the U.S. Northern Plains produced warm air temperature advection at 700 hPa and 850 hPa over northeastern Iowa and central Minnesota (Figs. 12c,d) that was collocated with a region of 7–14 cm storm total snowfall across southern and central Minnesota (not shown; Iowa State University 2019). Cold air temperature advection at 850 hPa over Lake Superior likely created steep lower-tropospheric lapse rates with sufficient static instability for the development of ELEnP over western Lake Superior (Fig. 12d). Warm air advection would later overspread the western Lake Superior region and influence the period of synoptic-enhanced ELEnP during the Type A-to-B transition (not shown).

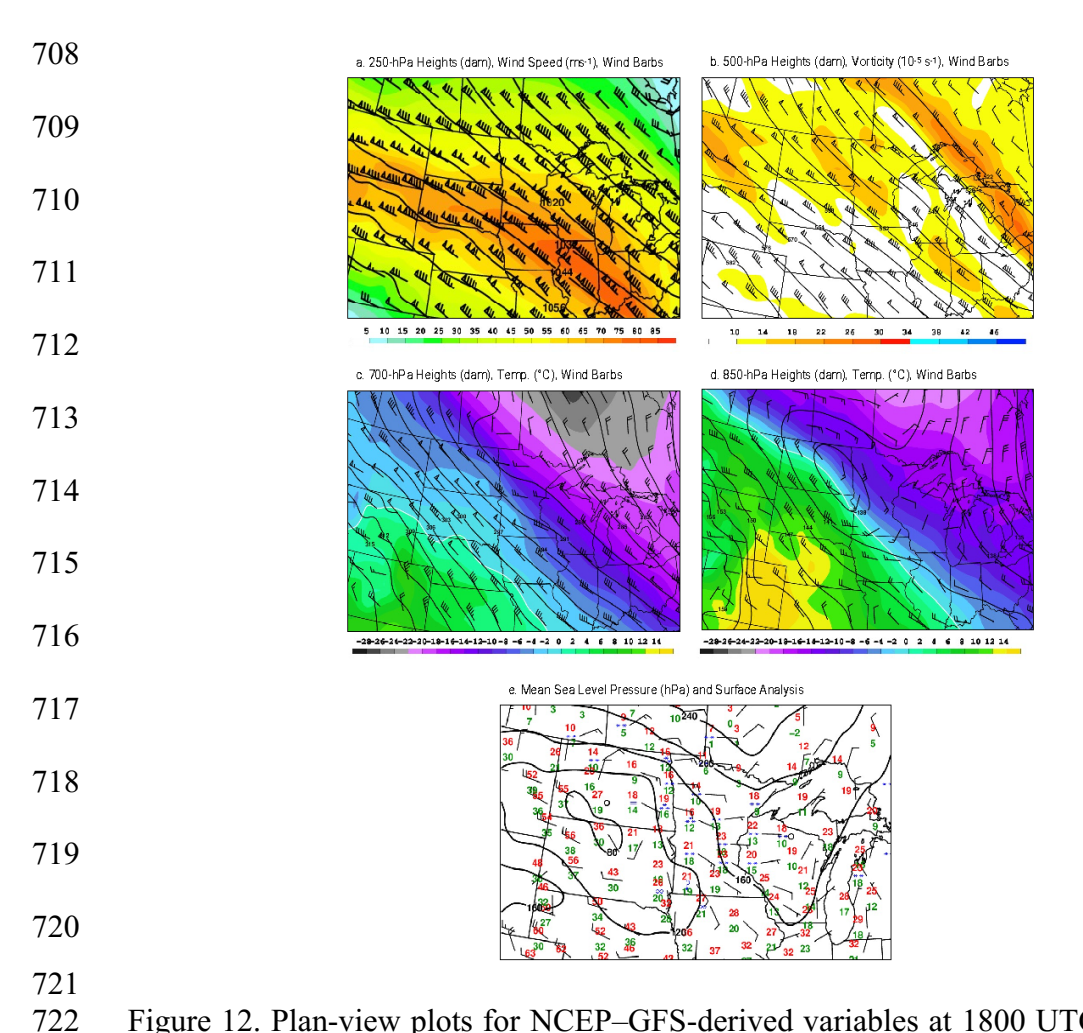


Figure 12. Plan-view plots for NCEP–GFS-derived variables at 1800 UTC 4 December 2007 a) 250-hPa geopotential height (dam; black contours), wind speed (m s<sup>-1</sup>; color fill) and wind velocities (flag =  $25 \text{ ms}^{-1}$ , barb =  $5 \text{ ms}^{-1}$ , half barb =  $2.5 \text{ ms}^{-1}$ ), (b) 500-hPa geopotential height (dam; black contours), absolute vorticity ( $10^{-5} \text{ s}^{-1}$ ; color fill for values > $10^{-4} \text{ s}^{-1}$ ), and wind velocities as in (a), (c) 700-hPa geopotential height (dam; black contours), temperature (C; color fill), and wind velocities as in (a), (d) as in (c) except for 850 hPa, and (e) SLP (hPa; contoured) with standard notation meteorological surface observations.

The ΔT between the lake water temperature and 850-hPa air temperature exceeded 20°C during the ELEnP event, with lake water temperatures of ~5°C and 850-hPa air temperatures of – 12 to -18°C. These values suggest that the boundary layer over western Lake Superior had the potential to become statically unstable and generate snowfall at an ideal temperature for dendritic growth (e.g., -12 to -18°C; Fuhrmann and Konrad 2013). Surface air temperatures of -18.9°C in northerly flow near Lake Nipigon to the north of Lake Superior and -6.7°C in easterly flow at KDLH suggest that Lake Superior modified the lower-tropospheric air mass to become convectively unstable in association with the development of the SB (D. J. Miller 2019, personal communication) in anticyclonic flow over western Lake Superior. An AMDAR aircraft sounding illustrates that the top of the lake-modified air mass was near 825 hPa concurrent with a temperature inversion and the upper extent of east-to-northeasterly winds (Fig. 13). A second inversion near the surface was likely due to low-level cold air advection, as shown by northerly winds near the surface (Fig. 13). A sounding from International Falls, MN, shows a low-level inversion topped at ~900 hPa, which is consistent with low-level cold air intruding at Duluth at this time (Fig. 14). The instability profile that must have been present over western Lake Superior was not sampled by the AMDAR sounding since the aircraft approached Lake Superior from the southwest; instead, downstream remnants of the unstable lake-modified air between ~900 hPa and 825 hPa are present (Fig. 13) with a land-based cold air advection layer below that (e.g., Fig. 14). The altitude of the top of the lake-modified air mass is consistent with radar echo tops derived from the radar reflectivity from KDLH. For example, the height of the 0.5° beam elevation at the location of the farthest ELEnP-related radar reflectivity >10 dBZ occurred at ~2100–2300 m AGL, which is consistent with echo tops near ~825 hPa over western Lake Superior (not shown). Both NCEP-CFSR-derived 925-850-hPa directional wind shear values and AMDAR observations of surface-to-inversion directional wind shear values were <30 degrees over western Lake Superior, favoring a SB event (e.g., Niziol 1987).

729

730

731

732

733

734

735

736

737

738

739

740

741

742

743

744

745

746

747

748

749

750

751

752

753

754

755

756

757

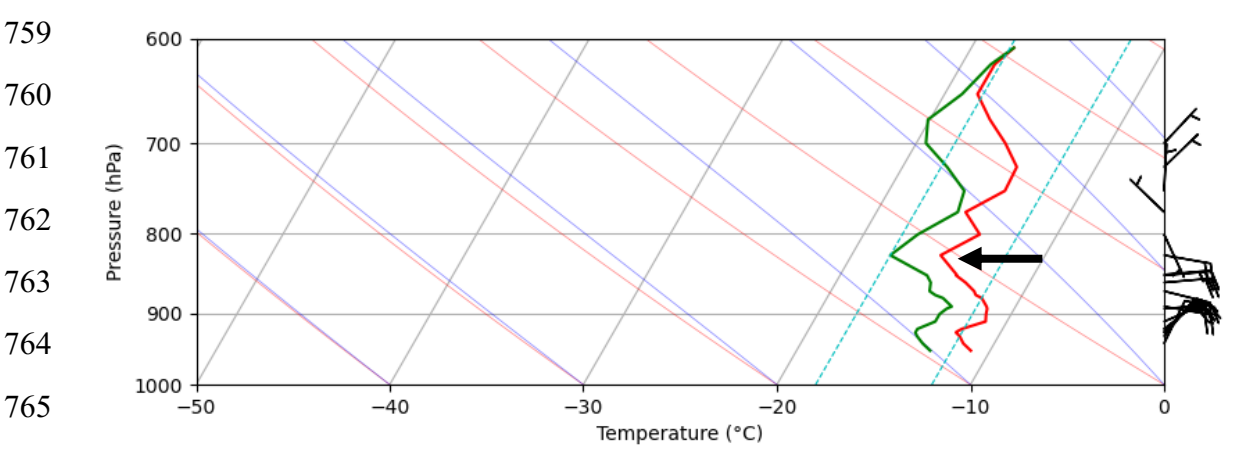


Figure 13. AMDAR aircraft-derived descent sounding at KDLH Airport at 0110 UTC 5 December 2007. The green line represents the dewpoint temperature and the red line represents the temperature. Blue dashed lines represent -12°C and -18°C isotherms indicative of the dendritic growth zone. The black arrow denotes a temperature inversion at ~825-hPa. Source: NOAA AMDAR page. Soundings were created using METPY (May et al. 2022).

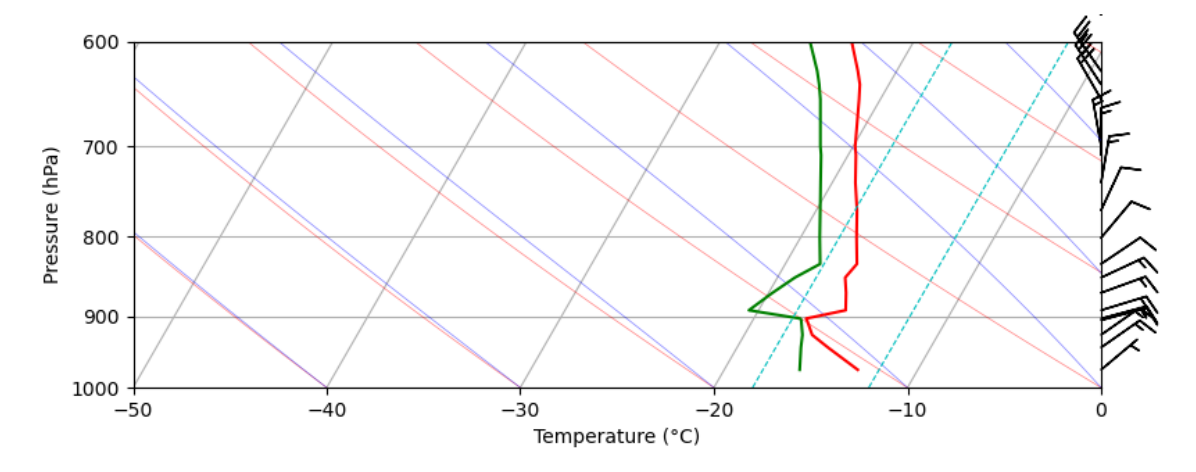


Figure 14. Atmospheric sounding from International Falls, Minnesota, at 0000 UTC 5 December 2007. The green line represents the dewpoint temperature and the red line represents the temperature. Blue dashed lines represent -12°C and -18°C isotherms indicative of the dendritic growth zone. Source: University of Wyoming. Soundings were created using METPY (May et al 2022).

As the synoptic-scale precipitation approached and became collocated with the ELEfP, the radar reflectivity values became enhanced (i.e., >20 dBZ) beginning at 1708 UTC, lasting for seven hours (Figs. 11d–f). Even with the synoptic precipitation shield filling in over Lake Superior, the ELEnP remained distinct on radar imagery. This enhancement of the band is consistent with synoptic enhancement of the ELEfP via the seeder–feeder mechanism (e.g.,

Waldstreicher 2002) and likely contributed to the localized snowfall totals of up to 43 cm (17 in; Fig. 10).

The predecessor SB ELEnP event that became enhanced by synoptic-scale precipitation as a Type A-to-B-to-A transition produced significant sensible weather impacts in the Twin Ports region due to intense snowfall rates and localized heavy accumulations in a well-populated area. Snowfall amounts of 43 cm and snowfall rates >5 cm h<sup>-1</sup> primarily occurred during the evening commute (Myers and Ashenmacher 2004). As such, people became stranded on area roadways for two hours with snowplows unable to clear roadways and traffic accidents closing a bridge connecting Minnesota and Wisconsin (Myers and Ashenmacher 2004). The high intensity, locality, and timing of the snowfall likely caught many commuters off guard, and poor preparation for the heavy snow may have been due in part to forecast uncertainty.

### 6. Discussion and Conclusion

Easterly wind episodes occur somewhat regularly over western Lake Superior with ~59.5 episodes per year. Easterly winds occur ~16.8% of the time between September and May. Despite their relatively infrequent occurrence, these easterly wind episodes occur in association with ~14–15 ELCP events per year over western Lake Superior, many of which impact the Twin Ports region of Northeast Minnesota. These ELCP events were most common during the months of December through February, with ELCP occurring ~58% of the time an easterly wind developed over western Lake Superior. Of these, ELEfP occurred during ~13% of easterly wind episodes. ELCP events primarily occur, on average, in association with a surface anticyclone located over southern Ontario and sometimes with a concurrent surface cyclone located to the south over the U.S. Central Plains and Midwest that favor geostrophic easterly flow over western Lake Superior. The majority of band types (n=97) were mixed-type events that featured transitions between band types owing to meso-synoptic interactions from passing surface cyclones and influences from synoptic precipitation that limited most ELCP events from retaining a uniform type for their entire duration. Given the concave western shoreline of Lake Superior, the most frequently observed uniform band type was SB events (n=60) closely followed by WNB events (n=49). The large number of SB events suggests that the concave shape of western Lake Superior organizes convection into a single band, likely with the aid of

land breeze convergence in a similar way that a westerly wind often produces SB events over Lake Ontario (e.g., Steenburgh and Campbell 2017).

The mixed-type ELCP events often featured transitions between band type owing to the influence of synoptic-scale precipitation (i.e., ELEnP). Herein, we define ELCP that occurred without any synoptic precipitation as Type A (i.e., ELEfP) and illustrated that these events primarily occurred in association with a surface anticyclone located to the north of Lake Superior that produced geostrophic easterly flow over western Lake Superior. ELCP that occurred with synoptic precipitation was defined as Type B (i.e., ELEnP) and occurred in association with both a surface anticyclone located to the north of Lake Superior and a surface cyclone located over the Central Plains and U.S. Midwest that combined favored geostrophic easterly flow over western Lake Superior. Type A events are hypothesized to primarily occur in association with lower-tropospheric cold air temperature advection that provides the convective instability necessary for ELEfP formation over western Lake Superior, whereas Type B events are hypothesized to occur in association with a combination of relatively weaker lower-tropospheric cold air advection that leads to ELEnP formation and advancing lower-to-mid-tropospheric warm air temperature advection that produces overrunning synoptic-scale precipitation.

The prevalence of Type B ELEnP events and transitions related to Type A-to-B events herein referred to as "predecessor ELEnP events" illustrates how many events occur in conjunction with synoptic-scale precipitation that may lead to an enhancement of ELEfP through the seeder-feeder mechanism. The seeder-feeder mechanism appears to occur frequently in association with ocean-effect or lake-effect precipitation that may develop in association with easterly flow that may occur within an environment characterized by an advancing region of low-pressure and warm air advection (e.g., Waldstreicher 2002; Owens et al. 2017). It is therefore hypothesized that many of these types of ELCP events that occur in association with synoptic-scale precipitation may not have occurred without the presence of synoptic-scale precipitation (i.e., ELEnP) or, if already developed, may occur in conjunction with heavier-than-expected lake-effect precipitation or greater storm (both ELEfP and synoptic-scale) total precipitation. An example of the former occurred during the Groundhog Day Blizzard of 2011, with 21%–23% of a ~54 cm (21.2 in.) storm total snowfall at Chicago-O'Hare Airport attributed to lake-enhancement from Lake Michigan (Owens et al. 2017). An example of the latter occurred in association with ~17 cm of ocean-effect snowfall and ~64 cm of synoptic-scale snowfall in

Portland, Maine, prior to and during a cyclone over the U.S. Northeast in early February 2013 (M. Clair 2019, personal communication). The combined snowfall totals resulted in a record storm-total snowfall that would not have occurred in the absence of the ocean-effect snowfall. The 4 December 2007 heavy snow event presented above also fits within this category.

The forecast implications of ELEfP over western Lake Superior share similarities to those of lake-effect precipitation over the eastern Great Lakes. For example, forecasts of ELEfP should focus on convective instability, vertical wind shear, lower-tropospheric wind speeds, fetch, boundary layer depth, and the role of synoptic-scale processes in modulating ELEfP morphology. In the present study, the general rule of  $\Delta T$  between the lake water temperature and 850-hPa air temperature of >13°C held during most ELEfP events. As with traditional thermodynamic ingredients, wind speed and directional wind shear ingredients identified in previous studies of lake-effect precipitation (e.g., Niziol 1987) are similar with ELEfP events over western Lake Superior, with ELEfP often associated with boundary-layer wind speeds  $\geq 5$  m s<sup>-1</sup> and directional wind shear <30 degrees. In addition, surface anticyclones centered north of western Lake Superior often produce cold east to northeasterly flow, which is favorable for ELEfP.

There are several distinctions for forecasting ELEnP over western Lake Superior versus ELEfP. The role of synoptic-scale processes in modulating ELEnP morphology should focus on an advancing cyclone over the U.S. Upper Midwest creating warm air advection that may produce synoptic-scale precipitation that could enhance lake-effect precipitation via the seeder-feeder mechanism. Owens et al. (2017) demonstrated that the lake-modified lower-tropospheric boundary in lake-enhanced precipitation may typically be shallower than pure lake-effect (e.g., a depth of ~1 km), as was the case during the 2011 Groundhog Day Blizzard. A similar finding was presented by Sanders (2017), where ELEnP sometimes developed with ΔT less than 13°C as convective instability likely existed in a shallower lower-tropospheric layer. Such events may involve a conditionally unstable lower-atmospheric thermal profile such that synoptic precipitation is the mechanism by which lake-effect processes are activated and storm-total precipitation is enhanced. The 4 December 2007 case study, which is a more extreme example of ELEfP that later became synoptically enhanced (i.e., Type A-to-B; ELEnP), represented a more unstable lower-atmosphere with an inversion height ~850–800-hPa. Since most ELEnP events featured lighter precipitation, this heavy snow case suggests that ~850–800-hPa may be the

highest that the base of capping inversions typically reach in ELEnP events over western Lake Superior, so it may be useful to evaluate the convective instability and vertical wind shear at lower altitudes, especially during cases occurring in the presence of lower-tropospheric warm air advection increasing temperatures at the 850-hPa level.

This study of ELCP events over western Lake Superior motivates expanding research on the frequency of ELCP over the remaining Great Lakes and U.S. Northeast coastline (i.e., oceaneffect) and its influence on climatological precipitation and high-impact weather events (e.g., Waldstreicher 2002; Owens et al. 2017; Sanders 2017). Since this introductory climatology of easterly wind enhanced precipitation influences owing to Lake Superior were treated collectively for much of this study (i.e., ELCP), additional research on ELEfP and ELEnP treated separately is warranted. Analysis of orographically enhanced ELCP over western Lake Superior (e.g., Gowan et al. 2022) due to a terrain ridge along the western shoreline of Lake Superior (Fig. 1) was not considered in this study. Additional research on precipitation contributions owing to orographic- versus lake-enhancement in ELCP events along the western Great Lakes may improve forecasting techniques. It is also worth noting that a majority ( $\sim$ 75%) of easterly wind episodes in this study did not produce ELCP during the cold season and identifying the characteristics of the ELCP ingredients that differentiate between those that produce ELCP and those that do not produce ELCP could be beneficial to forecasting. In addition, an examination of the societal impacts, or lack thereof, of ELCP events may improve messaging criteria by the NWS and other media outlets to better prepare people for the unique risks associated with a relatively infrequent, but potentially high-impact or ill-timed ELCP event (e.g., DeVoir 2004).

896897

898

876

877

878

879

880

881

882

883

884

885

886

887

888

889

890

891

892

893

894

895

### Acknowledgements

- A majority of the research supporting this manuscript was completed as a M.S. thesis at
- Plymouth State University by author Sandstrom in June 2020. Subsequent research supported by
- 901 NSF Award AGS- 2040594 awarded to the author Metz. Three anonymous reviewers greatly
- 902 improved the quality of this manuscript.

903

904

# **Data Availability Statement**

- The climatology of ELCP and related data associated with this study can be found in Sandstrom
- 906 (2020, p. 119–127).

907 References 908 909 AMS 2018: Definition for lake-effect snow. Accessed 20 July, 2018. [Available online at 910 http://glossary.ametsoc.org/wiki/Lake-effect snow]. 911 AMS 2018: Definition for seeder-feeder. Accessed 24 July, 2018. [Available online at 912 913 http://glossary.ametsoc.org/wiki/Seeder-feeder]. 914 915 Brusky, E. S., and T. D. Helman, 1991: An Excessive Lake-Enhanced Snowfall Episode over 916 Northeast Wisconsin on December 13-15, 1989. Central Region Technical Attachment 917 91-23. https://repository.library.noaa.gov/view/noaa/30226. 918 919 Campbell, L. S. and W. J. Steenburgh, 2017: The OWLeS IOP2b Lake-Effect Snowstorm: 920 Mechanisms Contributing to the Tug Hill Precipitation Maximum. Mon. Wea. Rev., 145, 921 2461–2478, https://doi.org/10.1175/MWR-D-16-0461.1. 922 923 Carruthers, D. J. and T. W. Choularton, 1983: A model of the feeder-seeder mechanism of 924 orographic rain including stratification and wind-drift effects. *Quart. Journal of the Roy*. 925 Meteor. Society, 109, 575-588. 926 927 Cordeira, J. M. and N. F. Laird, 2008: The Influence of Ice Cover on Two Lake-Effect Snow 928 Events over Lake Erie. Mon. Wea. Rev., 136, 2747–2763, 929 https://doi.org/10.1175/2007MWR2310.1. 930 931 DeVoir, G. A., 2004: High impact sub-advisory snow events: The need to effectively communicate the threat of short duration high intensity snowfall. Preprints, 20th Conf. on 932 933 Weather Analysis and Forecasting, Seattle, WA, Amer. Meteor. Soc., P10.2. [Available 934 online at https://ams.confex.com/ams/pdfpapers/68261.pdf]. 935 936 Eichenlaub, V. L., 1970: Lake effect snowfall to the lee of the Great Lakes: Its role in Michigan. 937 Bull. Amer. Meteor. Soc., **51**, 403-412. 938 939 Forbes, G. S., and J. H. Merritt, 1984: Mesoscale vortices over the Great Lakes in wintertime, 940 Mon. Wea. Rev., 112, 337–381, https://doi.org/10.1175/1520-941 0493(1984)112<0377:MVOTGL>2.0.CO;2. 942 943 Fuhrmann, C. M., and C. E. Konrad II, 2013: A Trajectory Approach to Analyzing the 944 Ingredients Associated with Heavy Winter Storms in Central North Carolina, Wea. 945 Forecasting, 28, 647-667, https://doi.org/10.1175/WAF-D-12-00079.1. 946 947 Gowan, T. M., Steenburgh, W. J., & Minder, J. R., 2022: Orographic Effects on Landfalling 948 Lake-Effect Systems, Mon. Wea. Rev., 150, 2013-2031, https://doi.org/10.1175/MWR-

Great Lakes Environmental Research Laboratory (GLERL), cited 2022: Great Lakes Ice Cover

Data – Ice Year 2008. Accessed 14 October 2022. [Available online at

949

950951

952

D-21-0314.1.

953	https://www.glerl.noaa.gov/data/pgs/glicd/glicd_2008.html].
954	
955	Grim, J. A., N. F. Laird, and D. A. R. Kristovich, 2004: Mesoscale vortices embedded within a
956	lake-effect shoreline band. Mon. Wea. Rev., 132, 2269-2274,
957	https://doi.org/10.1175/1520-0493(2004)132<2269:MVEWAL>2.0.CO;2.
958	
959	Hjelmfelt, M. R., 1990: Numerical Study of the Influence of Environmental Conditions on Lake-
960	Effect Snowstorms over Lake Michigan. Mon. Wea. Rev., 118, 138–150,
961	https://doi.org/10.1175/1520-0493(1990)118<0138:NSOTIO>2.0.CO;2.
962	
963	Holroyd, E. W., III, 1971: Lake-effect cloud bands as seen from weather satellites. J. Atmos. Sci.,
964	28, 1165-1170, doi: https://doi.org/10.1175/1520-
965	0469(1971)028<1165:LECBAS>2.0.CO;2.
966	
967	Iowa State University, cited 2022: Area Forecast Discussion National Weather Service Duluth
968	MN. Accessed 10 October 2022. [Available online at
969	https://mesonet.agron.iastate.edu/wx/afos/p.php?pil=AFDDLH&e=200802060847].
970	
971	Iowa State University, cited 2022: Area Forecast Discussion National Weather Service Duluth
972	MN. Accessed 10 October 2022. [Available online at
973	https://mesonet.agron.iastate.edu/wx/afos/p.php?pil=AFDDLH&e=200802070332].
974	
975	Iowa State University, cited 2022: Preliminary Local Storm Report National Weather Service
976	Duluth MN. Accessed 10 October 2022. [Available online at
977	https://mesonet.agron.iastate.edu/wx/afos/p.php?pil=LSRDLH&e=200802061813].
978	
979	Iowa State University, cited 2019: Public Information Statement National Weather Service
980	Duluth MN. Accessed 25 August 2019. [Available online at
981	https://mesonet.agron.iastate.edu/wx/afos/p.php?pil=PNSDLH&e=200712051759].
982	impontinessimus accommon accom
983	Kunkel, K.E., N.E. Westcott, D.A. Kristovich 2002: Assessment of potential effects of climate
984	change on heavy lake-effect snowstorms near Lake Erie. J. Great Lake. Res., 28 (4)
985	(2002), pp. 521-53
986	(2002), pp. 021 05
987	Kristovich, D. A. R., 1993: Mean circulations of boundary-layer rolls in lake-effect snow storms.
988	BoundLayer Meteorol. <b>63</b> , 293–315, https://doi.org/10.1007/BF00710463.
989	Bound. Bayer increases. 30, 255 313, increase and increas
990	Lackmann, G. M., 2001: Analysis of a surprise western New York snowstorm. Wea.
991	Forecasting, 16, 99–116, https://doi.org/10.1175/1520-
992	0434(2001)016<0099:AOASWN>2.0.CO;2.
993	<u>0434(2001)010&lt;0099.AOA3W1V22.0.CO,2</u> .
994	Laird, N. F., D. A. R. Kristovich, and J. E. Walsh, 2003: Idealized model simulations examining
995	the mesoscale structure of winter lake-effect circulations. <i>Mon. Wea. Rev.</i> , <b>131</b> , 206–221,
996	https://doi.org/10.1175/1520-0493(2003)131<0206:IMSETM>2.0.CO;2.
997	1000000000000000000000000000000000000
998	Laird, N. F., J. Desrochers, and M. Payer, 2009: Climatology of Lake-Effect Precipitation Events
110	Land, 14. 1., 3. Desiredicts, and 14. 1 ayer, 2007. Chinatology of Lake-Effect 1 recipitation Events

999 over Lake Champlain. J. Appl. Meteor. Climatol., 48, 232–250, 1000 https://doi.org/10.1175/2008JAMC1923.1. 1001 1002 Laird, N. F., N. D. Metz, L. Gaudet, C. Grasmick, L. Higgins, C. Loeser, and D. A. Zelinsky, 1003 2017: Climatology of cold season lake-effect cloud bands for the North American Great 1004 Lakes. Int. J. Climatol, 37, 2111–2121, https://doi.org/10.1002/joc.4838. 1005 1006 Lang, C. E., McDonald, J. M., Gaudet, L., Doeblin, D., Jones, E. A., and Laird, N. F. (2018). The 1007 influence of a Lake-to-Lake connection from Lake Huron on the lake-effect snowfall in 1008 the vicinity of Lake Ontario. J. Appl. Meteorol. Climatol. 57, 1423–1439. doi: 1009 10.1175/JAMC-D-17-0225.1 1010 1011 Liu, A. O., and G. W. K. Moore, 2004: Lake-effect snowstorms over southern Ontario, Canada, 1012 and their associated synoptic-scale environment. Mon. Wea. Rev., 132, 2595-2609, 1013 doi:10.1175/MWR2796.1. 1014 1015 May, R. M., Goebbert, K. H., Thielen, J. E., Leeman, J. R., Camron, M. D., Bruick, Z., Bruning, 1016 E. C., Manser, R. P., Arms, S. C., and Marsh, P. T., 2022: MetPy: A Meteorological 1017 Python Library for Data Analysis and Visualization. Bull. Amer. Meteor. Soc., 103, 1018 E2273-E2284, https://doi.org/10.1175/BAMS-D-21-0125.1. 1019 1020 Metz, N. D., Z. S. Bruick, P. K. Capute, M. M. Neureuter, E. W. Ott, and M. F. Sessa, 2019: An 1021 Investigation of Cold-Season Short-Wave Troughs in the Great Lakes Region and Their 1022 Concurrence with Lake-Effect Clouds. J. Appl. Meteor. Climatol., 58, 605-614, 1023 https://doi.org/10.1175/JAMC-D-18-0177.1. 1024 1025 Myers, J. and W. Ashenmacher, 2007: Heavy snow slams Duluth. Duluth News Tribune, 4 1026 December 2007. [Available online at 1027 https://www.duluthnewstribune.com/news/2254185-heavy-snow-slams-duluth]. 1028 1029 National Center for Atmospheric Research Staff (Eds). Last modified 08 Nov 2017. "The 1030 Climate Data Guide: Climate Forecast System Reanalysis (CFSR)." Retrieved from 1031 https://climatedataguide.ucar.edu/climate-data/climate-forecast-system-reanalysis-cfsr. 1032 1033 National Weather Service – Duluth, MN, cited 2019: NOWData – NOAA Online Weather Data. 1034 [Available online at <a href="https://w2.weather.gov/climate/xmacis.php?wfo=dlh">https://w2.weather.gov/climate/xmacis.php?wfo=dlh</a>]. 1035 1036 National Weather Service – Marquette, MI, cited 2019: NOWData – NOAA Online Weather 1037 Data. [Available online at https://w2.weather.gov/climate/xmacis.php?wfo=mqt]. 1038 1039 National Centers for Environmental Information, cited 2018: Climate Forecast System (CFS). 1040 [Available online at https://www.ncdc.noaa.gov/data-access/model-data/model-1041 datasets/climate-forecast-system-version2-cfsv2].

Nicosia, D. J., and Coauthors, 1999: A flash flood from a lake-enhanced rainband. Wea.

Forecasting, 14, 271-288, doi:10.1175/1520-0434(1999)014<0271:AFFFAL>2.0.CO;2.

1042 1043

1044

1045 1046 Niziol, T. A., 1987: Operational forecasting of lake effect snowfall in western and central New 1047 York. Wea. Forecasting, 2, 310-321, https://doi.org/10.1175/1520-1048 0434(1987)002<0310:OFOLES>2.0.CO;2. 1049 1050 Niziol, T. A., W. R. Snyder, and J. S. Waldstreicher, 1995: Winter weather forecasting 1051 throughout the eastern United States. Part IV: Lake effect snow. Wea. Forecasting, 10, 1052 61-77, https://doi.org/10.1175/1520-0434(1995)010<0061:WWFTTE>2.0.CO;2. 1053 1054 NOAA, 2022: WPC Surface Archive Page. Accessed 10 October 2022, 1055 https://www.wpc.ncep.noaa.gov/html/sfc-zoom.php. 1056 1057 NWS, 2015: Lake effect summary: November 17–19, 2014. NWSFO, Buffalo, NY. [Available 1058 online at www.weather.gov/buf/lake1415 stormb.html]. 1059 1060 Ogimet, cited 2019: Metar/Speci/Taf reports selection query. [Available online at 1061 https://www.ogimet.com/metars.phtml.en]. 1062 Owens, N. D., R. M. Rauber, B. F. Jewitt, and G. M. McFarquhar, 2017: The contribution of lake 1063 1064 enhancement to extreme snowfall within the Chicago-Milwaukee urban corridor during 1065 the 2011 Groundhog Day blizzard. Mon. Wea. Rev., 145, 2405-2420, 1066 https://doi.org/10.1175/MWR-D-17-0025.1. 1067 1068 Purdy, J. C., G. L. Austin, A. W. Seed, and I. D. Cluckie, 2005: Radar evidence of orographic 1069 enhancement due to the seeder feeder mechanism. Meteorol. Appl., 12, 199–206, 1070 doi:10.1017/S1350482705001672. 1071 1072 Sanders, M., 2017: Cold-season easterly wind events and associated lake-effect influences over 1073 the Eastern Great Lakes. B.S. Thesis, Department of Geoscience, Hobart and William 1074 Smith Colleges, 65 pp. 1075 1076 Sandstrom, J., 2020: A Climatology of Easterly Wind Lake-Effect Precipitation Events over the 1077 Western Lake Superior Region. M.S. Thesis. Applied Meteorology Program, Plymouth 1078 State University, 133 pp. 1079 1080 Schneider, D., and M. Moneypenny, 2002: The mesoscale seeder-feeder mechanism: Its forecast 1081 implications, Nat. Wea. Digest, 26(12), 45-52. 1082 1083 Schmidlin, T. W., 1993: Impacts of Severe Winter Weather during December 1989 in the Lake 1084 Erie snowbelt. J. Climate, 6, 759–767, https://doi.org/10.1175/1520-1085 0442(1993)006<0759:IOSWWD>2.0.CO;2. 1086 1087 Steenburgh, W. J., and L. S. Campbell, 2017: The OWLeS IOP2b Lake-Effect Snowstorm: 1088 Shoreline Geometry and the Mesoscale Forcing of Precipitation. Mon. Wea. Rev., 145, 1089 2421-2436, https://doi.org/10.1175/MWR-D-16-0460.1.

1090	
1091	Steiger, S. M., R. Schrom, A. Stamm, D. Ruth, K. Jaszka, T. Kress, B. Rathbun, J. Frame, J.
1092	Wurman, and K. Kosiba, 2013: Circulations, bounded weak echo regions, and horizontal
1093	vorticies observed within long-lake-axis-parallel lake-effect storms by Doppler on
1094	Wheels. Mon. Wea. Rev., 141, 2821–2840, https://doi.org/10.1175/MWR-D-12-00226.1.
1095	
1096	Wang, J., J. Kessler, F. Hang, H. Hu, A. H. Clites, and P. Chu, 2017: Great Lakes ice
1097	climatology update of winters 2012–2017: Seasonal cycle, interannual variability,
1098	decadal variability, and trend for the period 1973-2017. NOAA Tech. Memo. GLERL-
1099	170, 14 pp., <a href="https://www.glerl.noaa.gov/pubs/tech_reports/glerl-170/tm-170.pdf">https://www.glerl.noaa.gov/pubs/tech_reports/glerl-170/tm-170.pdf</a> .
1100	
1101	Waldstreicher, J. S., 2002: A foot of snow from a 3000-foot cloud: The Ocean-Effect Snowstorm
1102	of 14 January 1999. Bull. Amer. Meteor. Soc., 83, 19–22.
1103	
1104	Woolley, R., R. Caiazza, and T. A. Galetta, 1992: "Tea-kettle" effect snow. Proc. 49th Annual
1105	Eastern Snow Conf., Oswego, NY, U.S. Army, CRREL, 89-100.
1106	